A STUDY OF CD ELONGATION OF CORE IN WINDING

by

M. Ilomäki[1] and M. Jorkama[2]
Ahlstrom[1] Cores Oy
Metso[2] Paper, Inc.
FINLAND

ABSTRACT

In this paper the elongation of a core in a roll bottom is studied experimentally and theoretically. The CD elongation effects are of interest especially because they are known to contribute prominently to a two-drum winder vibration or roll instability phenomenon called *bouncing* in the paper industry.

Analytical and numerical calculation models are used to study the effect of different geometrical, material, etc., parameters on the core and paper CD elongation. If the free lateral elongation and rotation is allowed and the friction between paper and the core is neglected, the radial and tangential stresses of the core are due to the radial pressure only. The lateral and shear stresses are equal to zero and the elongation depends on the pressure, Poisson's ratios in the thickness-machine and thickness-cross directions, elastic modulus in the thickness and tangential directions and the geometry. If the lateral frictional forces between the paper and core are also taken into account, another, equally effective elongation mechanism is introduced.

The measurements of the paper and core elongation are in accordance with the calculated results. In practice, cores expand typically +/-1 mm/m depending on the tightness of the roll bottom and core properties. This study shows that the core elongation increases linearly with the radial pressure. Small diameter cores lengthen less than large cores. Cores with thicker wall thickness lengthen less than thinner cores, and cores with a bigger winding angle lengthen less than cores with a smaller winding angle (conventional cores).

The radial moduli of paper and the core wall also play an important role in the elongation of the core. Preliminary studies suggest that the softer the paper the more it tends to widen. According to paper stack modulus measurements, the radial modulus of paper layers in the roll bottom can be less than 100 MPa, even with high winding pressures. The radial elastic modulus of the core wall is usually 100 - 200 MPa or even

greater depending on the core type. It is possible that the frictional force between the core and paper could force the core to elongate more than it would without paper.

NOMENCLATURE

a=inner core radius, mm
b=outer core radius, mm
c=radial ratio
h=core wall thickness, mm
k=anisotropy ratio
p=internal pressure, MPa
q=external pressure, MPa
r=core radius, mm
r= radial direction core coordinate
z=longitudinal direction core coordinate

C=stiffness matrix term
E=Young's modulus
G=shear modulus
L=initial core length, mm
S =compliance matrix term

α =winding angle of board ply
ε =strain component
ν=Poisson's ratio
σ=normal stress
τ = shear stress
γ=shearing strain
θ =polar angle or direction
θ=tangential direction core coordinate

i, j=lower indexes referring to principal coordinates 1, 2 or 3
1=thickness direction board or paper coordinate
2=machine direction board or paper coordinate
3=cross-machine direction board or paper coordinate

GENERAL

Core elongation and paper widening can sometimes cause vibration problems, especially with two-drum winders. Adjacent rolls rotating at high angular velocity start to interact via the roll edges as the paper widens and the cores elongate. In some modern constructions the axial position of the chucks is force controlled to avoid such problems. Excessive axial forces can cause core bending and vibration problems. The problems become even worse if the core ends are not cut straight. As a consequence of this the vibration levels of the rotating rolls and the paper web increase, which typically increases the number of web breaks. It has been seen in practice that the problem becomes worse when winding certain bulky paper grades.

CONSIDERATIONS OF BOARD AND PAPER

The material behavior of typical core boards (and papers) is in general very complex with nonlinear elastic and viscoelastic features. The linear elastic modulus is determined in the beginning of the stress-strain curves (greatest slope). If the applied stress is less than 40 % of the breaking stress and the tensile speed is no less than say 10 - 20 mm/min, the material behavior of a representative, typical board is still quite linear and elastic.

Board and paper are usually considered as orthotropic materials and, hence have three principal material directions. Orthotropic materials have two orthogonal symmetry planes for the elastic properties [1]. Symmetry will exist also relative to a third mutually orthogonal plane. For linear, elastic material there are only nine independent material constants in the stiffness matrix. There is no interaction between normal stresses σ_i and shearing strains γ_{ij} in the principal material coordinates. Similarly, there is no interaction between shearing stresses τ_{ij} and normal strains ε_i, as well as none between shearing stresses and shearing strains in different planes [2]. Considering generalized Hooke's law for orthotropic material, the strain-stress relations are [1]

$$\begin{pmatrix} \varepsilon_1 \\ \varepsilon_2 \\ \varepsilon_3 \\ \gamma_{12} \\ \gamma_{13} \\ \gamma_{23} \end{pmatrix} = \begin{pmatrix} S_{11} & S_{12} & S_{13} & 0 & 0 & 0 \\ S_{12} & S_{22} & S_{23} & 0 & 0 & 0 \\ S_{13} & S_{23} & S_{33} & 0 & 0 & 0 \\ 0 & 0 & 0 & S_{44} & 0 & 0 \\ 0 & 0 & 0 & 0 & S_{55} & 0 \\ 0 & 0 & 0 & 0 & 0 & S_{66} \end{pmatrix} \cdot \begin{pmatrix} \sigma_1 \\ \sigma_2 \\ \sigma_3 \\ \tau_{12} \\ \tau_{13} \\ \tau_{23} \end{pmatrix} \tag{1}$$

The compliance $[S_{ij}]$ matrix is the inverse of the stiffness $[C_{ij}]$ matrix and the strain-stress relations in terms of engineering constants in the principal material directions 1, 2 and 3 are [1]

$$\begin{pmatrix} \varepsilon_1 \\ \varepsilon_2 \\ \varepsilon_3 \\ \gamma_{12} \\ \gamma_{13} \\ \gamma_{23} \end{pmatrix} = \begin{pmatrix} \frac{1}{E_1} & -\frac{\nu_{21}}{E_2} & -\frac{\nu_{31}}{E_3} & 0 & 0 & 0 \\ -\frac{\nu_{12}}{E_1} & \frac{1}{E_2} & -\frac{\nu_{32}}{E_3} & 0 & 0 & 0 \\ -\frac{\nu_{13}}{E_1} & -\frac{\nu_{23}}{E_2} & \frac{1}{E_3} & 0 & 0 & 0 \\ 0 & 0 & 0 & \frac{1}{G_{12}} & 0 & 0 \\ 0 & 0 & 0 & 0 & \frac{1}{G_{13}} & 0 \\ 0 & 0 & 0 & 0 & 0 & \frac{1}{G_{23}} \end{pmatrix} \cdot \begin{pmatrix} \sigma_1 \\ \sigma_2 \\ \sigma_3 \\ \tau_{12} \\ \tau_{13} \\ \tau_{23} \end{pmatrix} \tag{2}$$

where E_1, E_2, E_3 are the Young's modulus (E-modulus) values, ν_{ij} are Poisson's ratios, G_{23}, G_{13}, G_{12} are the shear modulus values in the 2-3, 1-3 and 1-2 planes. Because of symmetry $S_{ij} = S_{ji}$, there are nine independent constants.

Figure 1 shows the principal board web and core coordinates. The three principal board web coordinates (1, 2 and 3) in this study, respectively, are the thickness direction (td), the machine direction (md) and the cross direction (cd). The properties of elasticity are different in each of the three principal directions. Coordinates of the natural directions of a core are the thickness or radial direction (r), the tangential direction θ and the longitudinal direction (z). It should be noted here that z-direction is not the thickness direction as in many other paper or board related articles. From figure 1 we can see that spiral cores are constructed in such a manner that the principal board web directions do not coincide with the principal core coordinates. The principal board web directions 2 and 3 are rotated around direction 1 by winding angle α.

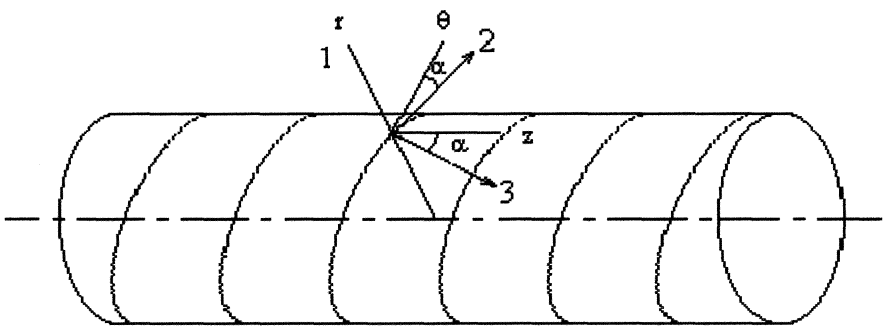

Figure 1. The principal board web and core coordinates.

E-modulus

The machine direction E-modulus of most common boards for paper industry cores is usually in the range of 4000 – 7000 MPa and the md/cd modulus ratio is approximately 1.5 – 2.5. The E-modulus of many paper grades is also within this range. Table 1 shows as an example, the longitudinal E-modulus of Ahlstrom cores.

core	Nomal core E [MPa]	New M-core E [MPa]
76x15	V5 (E=4000)	
76x15	V6 (E=4500–4700)	V5M (E=5500-5700)
76x15	V7 (E=4700)	V6M (E=5700)
150x13	V6 (E=4000)	V6M (E=4800-4900)
150x13	V7 (E=4000)	V7M (E=5500-5700)

Table 1. longitudinal E-modulus of Ahlstrom cores

Figure 2 shows the compressibility of example paper layers as a function of compressive pressure. The compression E-moduli of glued board stacks and core wall samples are shown in figure 3. The compression behavior of core wall samples and glued board stacks are more linear than that of paper stacks. This is because the board layers have already been heavily compressed together during the gluing process. We can say that in practice, the core wall compresses linearly as a function of pressure. After several compression cycles over the limit of elasticity, the density and compression E of board and paper could increase somewhat further. Figures 2 and 3 show that depending on the winding tightness and the paper & core grade, there can be differences between compressibility of paper at reel bottom and the core wall.

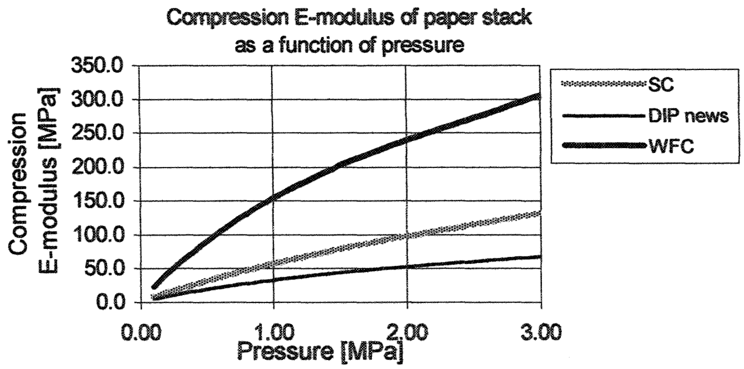

Figure 2. Compression E-modulus of example papers as a function of compression pressure. Density of papers SC (1.11 g/m3), DIP news (0.74 kg/m3), WFC (1.32 g/m3).

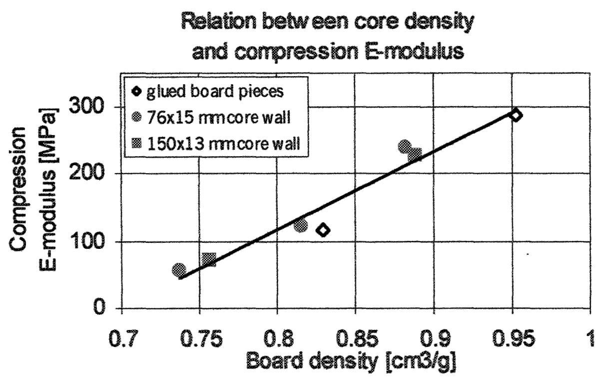

Figure 3. Compression E-modulus of core walls and of glued core board samples.

<u>Poisson´s ratios</u>

Poisson´s ratio ν_{ij} for transverse strain in the j-direction when stressed in the i-direction can be written as [1]

$$\nu_{ij} = -\frac{\varepsilon_j}{\varepsilon_i} \qquad \text{for } \sigma_i = \sigma \quad \text{and} \quad \sigma_j = 0 \tag{3}$$

Tensile deformation is considered positive and compressive deformation negative. From the symmetry requirement of the compliance matrix ($S_{ij} = S_{ji}$) it follows that

$$\frac{\nu_{ij}}{E_i} = \frac{\nu_{ji}}{E_j} \qquad i, j = 1,2,3 \tag{4}$$

Using this relation, only ν_{12} , ν_{13} and ν_{23} needs to be measured, since ν_{21} , ν_{31} and ν_{32} can be calculated.

Determination of the Poisson´s ratios of paper and also of board by the direct measurements of stresses and strains is difficult. Uncertainty arises from non-uniformity of stress and strain within the region of measurement, the specimen dimensions, error in the strain measurement, the possibility of specimen "tension buckling" (wrinkles) under uniaxial tensile stress and inelastic contributions to the measured strain [7]. It is also possible to measure the Poisson ratios of board or paper by ultrasonic [3] or image analysis method [4]. We will next review two examples from literature to get an idea of the magnitude of the Poisson's ratios in these example situations.

J.Aliranta measured in reference [5] the (in-plane) $\nu_{machine\ cross}$ direction values for core boards using direct measurements. For board with $E_{machine}$ 6550 MPa, E_{cross} 2670 MPa and $E_{thickness}$ in the order of 120 MPa in compression, the measured $\nu_{machine\ cross}$ was of the order 0.3. The out of plane Poisson's ratios used were $\nu_{machine\ thickness}$ 3.35 , $\nu_{cross\ thickness}$ 2.4, $\nu_{thickness\ machine}$ 0.05 and $\nu_{thickness\ cross}$ 0.1.

In reference [3], R.W. Mann et al, determined the elastic constants for milk carton using ultrasonic methods. The Poisson's ratio in the machine-thickness direction was located in the range from 0.59 to 2.45. The Poisson's ratio in the cross-thickness direction was located in the range from 1.32 to 2.36. Some other measured values were $\nu_{machine\ cross}$ 0.32, $\nu_{cross\ machine}$ 0.15, $E_{machine}$ 7440 MPa, E_{cross} 3470 MPa and $E_{thickness}$ 39 MPa.

For our calculation studies we need representative core properties. We will use here the following material constant for waterglass glued board web in its principal material directions (1,2 and 3): E_1 = 130 MPa, E_2 = 6500 MPa, E_3 = 4000 MPa, G_{12}=343 MPa, G_{13}=234 MPa, G_{23} = 2200 MPa, ν_{23} = 0.3, ν_{21} = 2.4, ν_{31} = 3.0, ν_{32} = 0.185 , ν_{12} = 0.048, ν_{13} = 0.098. The E-modulus and shear modulus values have been measured and the out of plane Poisson ratios have been chosen based on the literature examples and material values. The magnitude of the out of plane Poisson's ratios are checked against the lengthening behavior of cores under external pressure. It was found that the constants and their relative magnitude are of the correct level.

LENGTHENING OF CORES UNDER EXTERNAL PRESSURE

Theoretical studies

Hamad [6] has studied the core under external pressure possessing cylindrical anisotropy. It has been assumed that the material follows the linear Hooke's law. The faces of the core are free from load. The core has constant thickness and the state of plane stress has been assumed. The principal material directions of the 2D-model are the radial (r) and tangential (θ) directions. Figure 4 shows such a core cross section under external pressure.

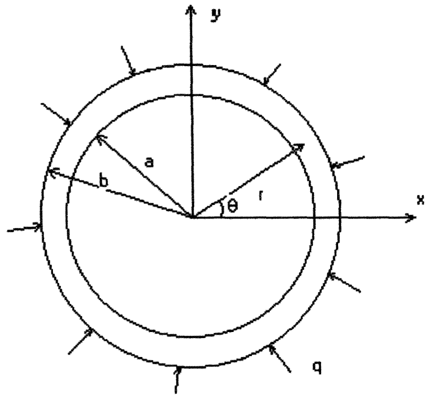

Figure 4. Core cross section with cylindrical anisotropy. θ is the polar angle and r represents the radius to any point inside the core cross section [6].

Distribution of radial and tangential stresses in core wall

The distribution of tangential σ_θ and radial σ_r stresses in the core wall under only external or both external and internal pressure will be studied next. In reference [6] it was shown that the equations of tangential and radial stresses of anisotropic cylinder under external and internal pressure load can be written as

$$\sigma_\theta = \frac{\left(p \cdot c^{k+1} - q\right)}{\left(1 - c^{2 \cdot k}\right)} \cdot k \cdot \left(\frac{r}{b}\right)^{(k-1)} + \left[\frac{p - q \cdot c^{(k-1)}}{1 - c^{2 \cdot k}}\right] \cdot k \cdot c^{(k+1)} \cdot \left(\frac{b}{r}\right)^{(k+1)} \tag{5}$$

$$\sigma_r = \frac{\left(p \cdot c^{k+1} - q\right)}{\left(1 - c^{2 \cdot k}\right)} \cdot \left(\frac{r}{b}\right)^{(k-1)} - \left[\frac{p - q \cdot c^{(k-1)}}{1 - c^{2 \cdot k}}\right] \cdot c^{(k+1)} \cdot \left(\frac{b}{r}\right)^{(k+1)} \tag{6}$$

where a and b denote the inner and outer radii of the core as in figure 1. The radial ratio $c = a / b$. The uniform pressure at the exterior core surface is denoted by q. The internal pressure is denoted by p. The radius to any point in the core cross section is denoted by r. The anisotropy ratio, k, is defined as

$$k = \sqrt{\frac{E_\theta}{E_r}} \tag{7}$$

where E_θ is the E modulus of the core material in the tangential direction. E_r is the E modulus of the core material in the thickness direction. The shear stress $\tau_{r\theta} = 0$. The equations for isotropic materials are evaluated by setting $k = 1$.

Figure 5 shows a comparison of tangential stresses, calculated analytically from equation (5) and by 2D-FEM model (Abaqus). The material constants are $E_\theta = 6100$ MPa and $E_r = 130$ MPa. The analytic and FEM plane stress results are identical. The plane strain stress distribution is slightly different than the plane stress distribution. The averages of the plane strain and plane stress distributions are the same. The distribution of radial stresses is linear and compressive (fig. 6). This distribution is the same for plane stress and plane strain solutions.

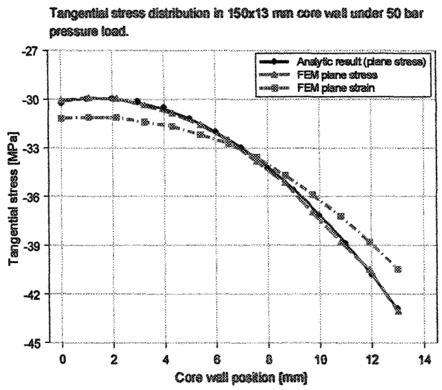

Figure 5. Tangential stresses σ_θ.

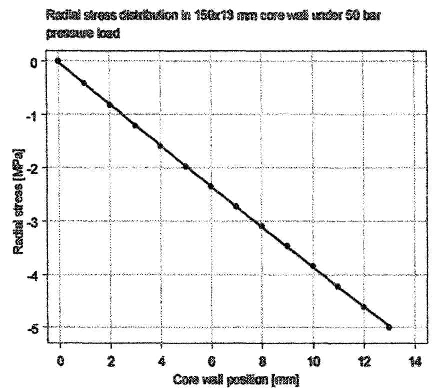

Figure 6. Radial stresses σ_r.

Longitudinal strain and lengthening of cores under external pressure

The equation of longitudinal strain of the core is evaluated from the stress strain relations. The average of longitudinal lengthening of a core is calculated by multiplying the average of axial strain in the core cross section by the initial core length. The averages of radial and circumferential stresses are needed in this calculation process.

It has been assumed that the paper and core are allowed to lengthen and rotate freely. This means that longitudinal and shear stresses are equal to zero. Applying the stress-strain relations of orthotropic material (eq. 2), we find, that the strain in the z-direction is written as

$$\varepsilon_z = \frac{-\nu_{rz}}{E_r}\cdot\sigma_r - \frac{\nu_{\theta z}}{E_\theta}\cdot\sigma_\theta \tag{8}$$

where the lower indexes refer to principal core coordinates r (radial), θ (tangential) and z (longitudinal), as in figure 1. σ_θ and σ_r as are calculated as in equations (5) and (6). The averages of radial and tangential stresses distributions are

$$\sigma_{raverage} = \frac{1}{h}\cdot\int_a^b \sigma_r\,dr \tag{9}$$

$$\sigma_{\theta average} = \frac{1}{h}\cdot\int_a^b \sigma_\theta\,d\theta \tag{10}$$

where h is the core wall thickness. Using the average stresses, the average strain in the core cross section is

$$\varepsilon_{zaverage} = \frac{-\nu_{rz}}{E_r}\cdot\sigma_{raverage} - \frac{\nu_{\theta z}}{E_\theta}\cdot\sigma_{\theta average} \tag{11}$$

The average lengthening of the core cross section is now

$$\Delta L_{average} = \varepsilon_{zaverage} \cdot L \quad (12)$$

where L is the initial core length. Examples of calculated results of the lengthening of 76x15 mm and 150x13 mm cores are shown in figures 7 – 14. The results have been calculated using the representative values for glued board web in its principal material coordinates: E_1 = 130 MPa, E_2 = 6500 MPa, E_3 = 4000 MPa, G_{12}=343 MPa, G_{13}=234 MPa, G_{23} = 2200 MPa, ν_{23} = 0.3, ν_{21} = 2.4, ν_{31} = 3.0, ν_{32} = 0.185 , ν_{12} = 0.048, ν_{13} = 0.098. The needed core properties have been calculated in the principal core coordinates as a function of the winding angle.

Cores are under external pressure and paper layers under external and internal pressure. The results show that cores usually lengthen less if there is only external pressure. Also, 75x15 mm cores lengthen less than 150x13 mm cores.

Figures 7 and 8 show the effect of the winding angle. The more oriented the example board md direction is to the core longitudinal direction, the less the cores lengthen. The measured results support this result as we will see later. Figures 9 and 10 give an idea of the effect of the thickness (radial) direction E-modulus of the core wall on core lengthening. The smaller the E-modulus, the greater is the effect. The less compressible the material, the less it should lengthen.

Figures 11 and 12 show also that the stiffer the core material is in the circumferential core coordinates, the less the core should lengthen. This effect is not as clear as that of the thickness direction E-modulus.

The calculated results in figures 9 – 12 are only indicative, since the effect of changing one material property on others has not been considered. For example, changing the thickness E-modulus could affect also the out of plane Poisson´s ratios. In any case, the variation has been done on a relatively narrow band.

Finally, figures 13 and 14 show the effect of E-modulus on the lengthening of isotropic cores. Here again we can see that the stiffer the material the less there is lengthening.

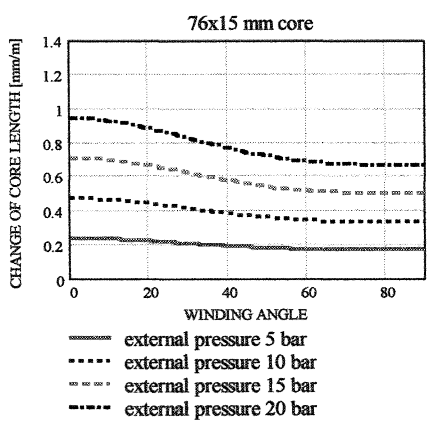

Figure 7. 76x15 mm core.

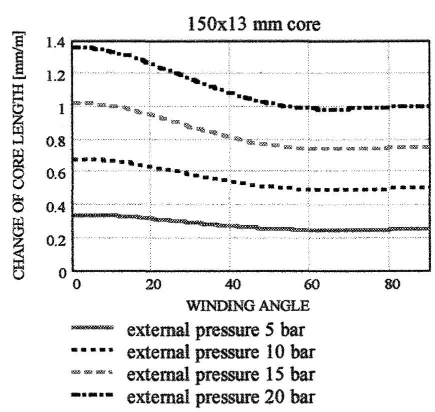

Figure 8. 150x13 mm core.

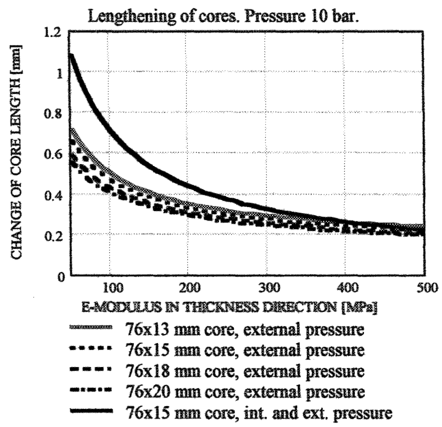

Figure 9. 76x15 mm core.

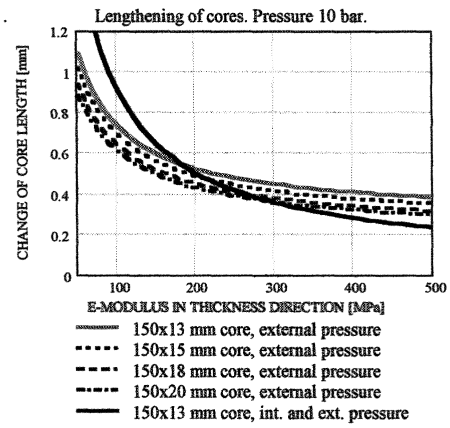

Figure 10. 150x13 mm core.

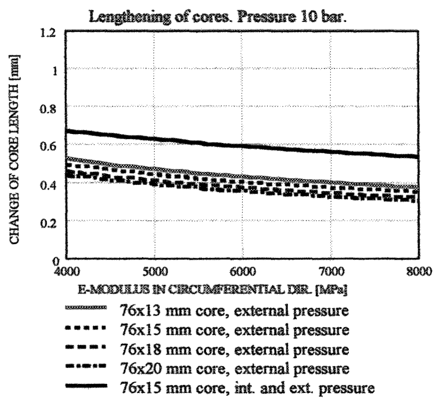

Figure 11. 76x15 mm core.

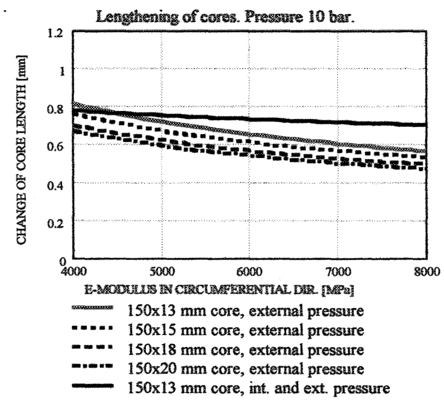

Figure 12. 150x13 mm core.

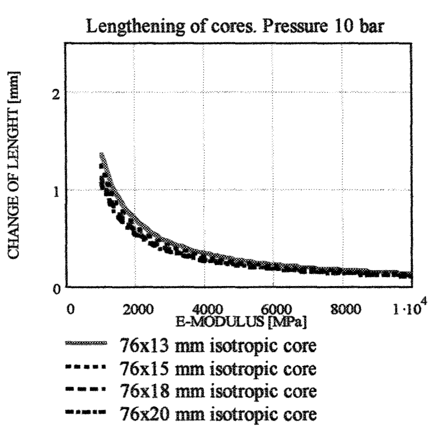

Figure 13. 76x15 mm isotropic core.

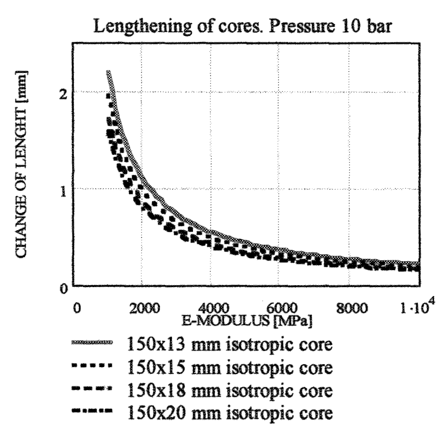

Figure 14. 150x13 mm isotropic core.

Practical studies

One important difference should be noted when comparing the measured and calculated results. The calculation equations consider only the pressure effect but not the friction interaction between the core and the paper layers. It is possible that in practice, the core and the paper layers have different lengthening tendencies but friction forces constrain their lengthening. This could explain some differences between the calculated and measured results of core lengthening.

Core lengthening has been measured in practice in paper mills and during test winder runs. The lengths of the cores have been measured before and after the winding process. Core length has been measured by using a tape measure as well as by a more accurate device as shown in figure 15. It is important to do the measurements from the same position before and after winding. Paper lengthening is, in general, more difficult to measure reliably.

Paper pressure on the core has been measured by using FlexiForce sensors or by measuring the change of the core's inside diameter during winding. Figure 16 shows the FlexiForce sensor on the core surface. If several sensors are attached on the same core there is usually some 20 % variation in the results as even small bumps on the core's surface could cause local variation in pressure distribution. The other methods to estimate the paper pressure are the pull-tabs and by measuring the change of the core's inside diameter.

Figure 17 shows the measured change of inside diameter of typical paper industry cores under external pressure. Figure 18 shows the correlation between measured and calculated results. The measured and calculated results are very much in accordance for 13-15 mm wall thickness. The smaller the wall thickness, the greater is the compressive tangential stress and the more non-linear is the behavior. This explains the deviation in the results with smaller wall thickness values. Analytical calculation model in reference [6] assumes linear elastic material behavior.

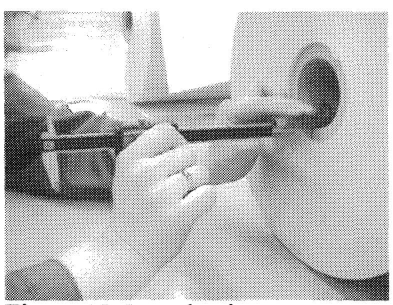

Figure 15. Lengthening measurement.

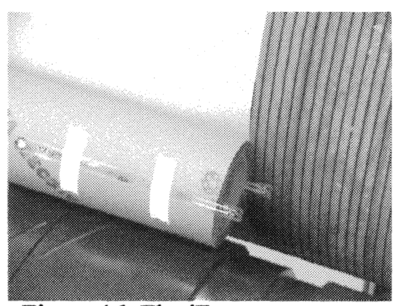

Figure 16. FlexiForce sensors

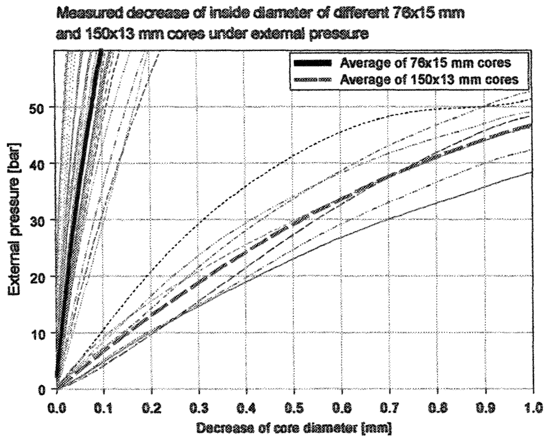

Figure 17. Measured results of different 76x15 and 150x13 mm cores. The results cover the most typical paper industry cores. The thick curves show the average of the test results. Non linear behavior increases along with pressure.

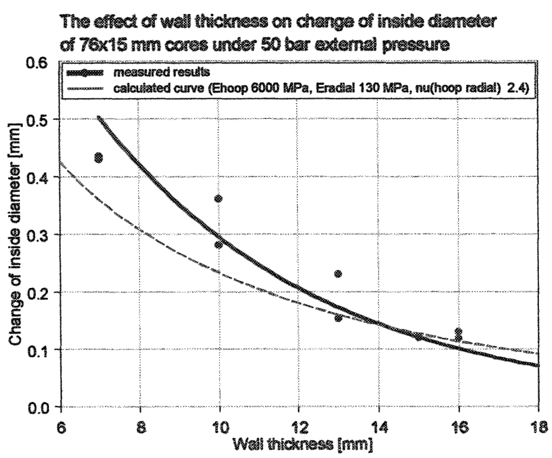

Figure 18. Measured and calculated results of changes to the core's inside diameter under external pressure. The material properties in the principal core coordinates are $E_\theta = 6000$ MPa, $E_r = 130$ MPa and $\nu_{\theta r} = 2.4$. Non-linear material behavior causes deviation in the calculated and measured results as the wall thickness becomes smaller.

Figure 19 shows an example of winding test results with a Winbelt test winder. The compression E-modulus of example papers as a function of compression pressure was shown in figure 2. The compression E-modulus of the test V5 and V5M cores was in the order of 130 - 150 MPa. Static friction between different papers and cores was 0.3 – 0.36. Static friction between paper layers was 0.4 – 0.5.

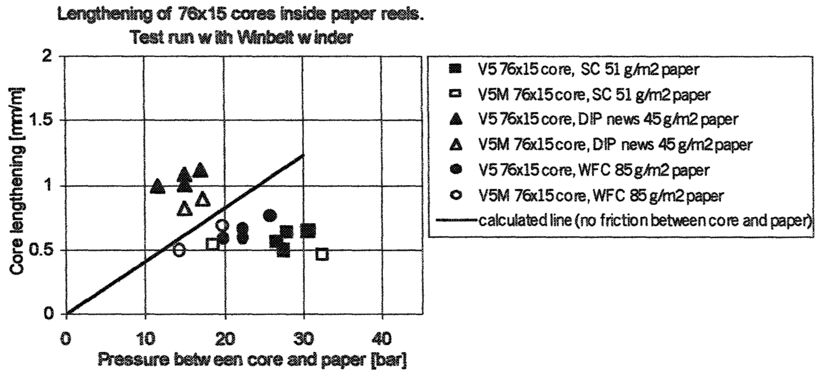

Figure. 19. Winding tests with 76x15 mm cores.

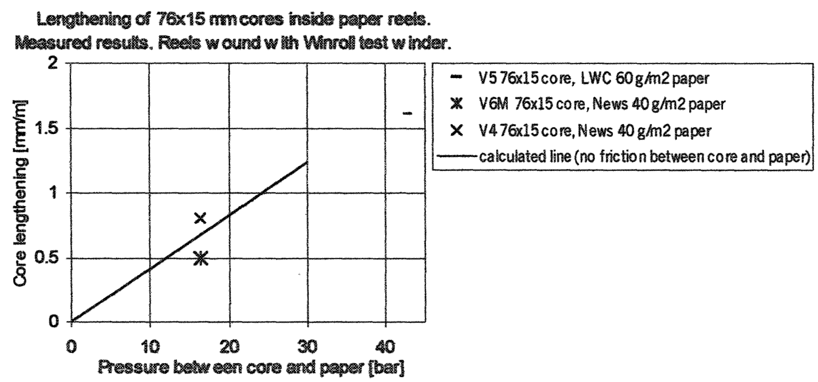

Figure. 20. Paper mill winder measurements of 76x15 mm cores.

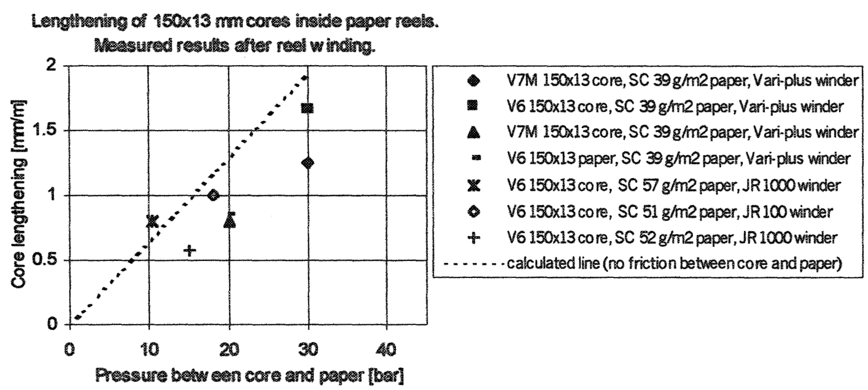

Figure. 21. Paper mill measurements of 150x13 mm cores.

Figures 20 and 21 show the results of measurements of the lengthening of cores in paper mills. There is a relatively good correlation between the calculated and measured results. From figures 19 and 20 we can see that that the M-cores with higher winding angle and longitudinal stiffness tend to lengthen less than conventional cores.

Some results from figure 21 have been collected in table 2. We can see that 150x13 mm cores with more winding angle lengthen less than conventional cores. The results are in accordance with the calculated results in figures 7 and 8. The winding angle has been explained in figure 1. The greater the winding angle of board plies, the more the board machine direction is oriented to the longitudinal core direction. This increases the core's stiffness in the longitudinal core coordinate, and affects also the Poisson's ratios in the principal core coordinates.

Winding angle	Winding pressure	
	20 bar	30 bar
18°	0.85	1.7
51°	0.8	1.3

Table 2. Measured effect of winding angle and winding pressure on lengthening of 150x13 mm cores

<u>Considerations of friction</u>

Depending on the properties of the paper and the core, it is possible that paper and cores might tend to lengthen differently. In problem cases the paper is typically more compressible than the core wall. A good example of this can be seen in the results in figure 19. Lengthening of cores with soft DIP news was more than what would have been expected from a pure pressure effect.

We could expect that friction forces between paper and core could affect core lengthening. If we use Coulomb's friction law, we can find that friction forces between core and paper are in many cases high enough to affect core lengthening. Even a relatively small coefficient of friction, such as 0.1 with some 15 bar winding pressure, is enough to transmit the necessary forces to stretch most cores.

REFERENCES

1. Abaqus 5.6 User's manual volume1. p. 10.2.1-2, Hibbit, Karlsson & Sorensen, Inc. 1996, p. 10.2.1-2
2. Jones, R.M., Mechanics of composite materials, Washington D.C. 1975, Scripta book company, p. 34, 35, 38.
3. G.A. Baum, D. C. Brennan, C. C. Habeger, Orthotropic elastic constants of paper, Tappi / August 1981, Vol 64, No. 8.
4. Markku Kujala, Isko kajanto, Paperin poissonin vakioitten määrittäminen kuva-analyysillä, KCL paper science centre publication 84, 24.11.1995.
5. Aliranta, Juha., Rakenneparametrien vaikutus kartonkihylsyn ominaisuuksiin, Diplomityö, Oulun Yliopisto 1988.
6. Wadood Hamad, Winding Mechanics of anisotropic materials, Pira technology series 1998
7. J. P. Brezinski, K. W. Hardacker, Poisson ratio values, Tappi / August 1982, Vol. 65, No. 8.